

Iridium Photocatalysts in Free Radical Photopolymerization under Visible Lights

Jacques Lalevée,^{*,†} Mohamad-Ali Tehfe,[†] Frédéric Dumur,[‡] Didier Gigmes,^{*,‡} Nicolas Blanchard,[§] Fabrice Morlet-Savary,[†] and Jean Pierre Fouassier^{||}

[†]Institut de Science des Matériaux de Mulhouse IS2M, LRC CNRS 7228, ENSCMu-UHA, 15, rue Jean Starcky, 68057 Mulhouse Cedex, France

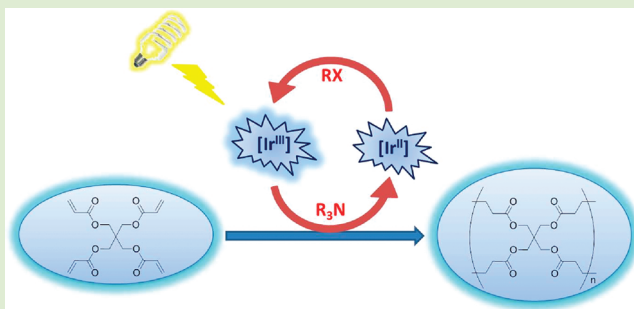
[‡]Laboratoire Chimie Provence UMR CNRS 6264, Equipe CROPS, Université de Provence, Avenue Escadrille Normandie-Niemen, Case 542, 13397 Marseille Cedex 20, France

[§]Laboratory of Organic and Bioorganic Chemistry, University of Haute Alsace, ENSCMu, 3 rue Alfred Werner, 68093 Mulhouse Cedex, France

^{||}UHA-ENSCMu, 3 rue Alfred Werner 68093, Mulhouse, France

S Supporting Information

ABSTRACT: A series of iridium(III) complexes was designed and investigated as new potential photocatalysts for radical polymerization reactions. The photocatalytic reduction cycle involves the combination of an iridium complex with an amine (e.g., *N*-methyldiethanolamine) and an alkyl halide (e.g., phenacylbromide). The different three-component systems herein investigated are very attractive for acrylate polymerization upon visible light irradiation. They are much more reactive than those based on $\text{Ru}(\text{bpy})_3^{2+}$. Free radicals generated during the reaction were investigated by ESR spectroscopy and the chemical mechanisms are discussed. The crucial role played by the photocatalyst (reduction ability and excited state lifetime) is also demonstrated.



Photoredox catalysis has clearly emerged in the synthetic community as a valuable strategy for the smooth generation of free radicals under very soft irradiation conditions (e.g., sunlight, household fluorescence or LED bulbs, and Xenon lamp).^{1–3} The use of $\text{Ru}(\text{bpy})_3^{2+}$ as a photocatalyst is now well-documented in organic chemistry. It is characterized by an excellent visible light absorption property and can work through either an oxidation or a reduction cycle.

Very recently, this photoredox catalysis approach was introduced into the polymer chemistry area to initiate a free radical promoted cationic photopolymerization (FRPCP) or a free radical photopolymerization. This novel way extends the development and the design of photoinitiators and photosensitizers for fast polymerization reactions (see, e.g., ref 4) usable in various applications.⁵ For example, Ru and Ir based complexes in combination with a silane and an iodonium salt work in FRPCP through an oxidation cycle.^{6,7} The Ru complex/amine/phenacyl halide system to initiate a polymerization reaction is presumably in this free radical polymerization area the first example of a photocatalyst that operates according to a reduction cycle^{6a} (where the $\text{Ru}(\text{bpy})_3^{2+}$ excited state reacts with a sacrificial quencher (the amine) to generate its reduced form ($\text{Ru}(\text{bpy})_3^+$), with this latter species being a strong reducing agent leading to the formation of carbon-

centered radicals by reaction with the halide). This system exhibits, however, a relatively low efficiency in free radical polymerization. In a more recent paper, a somewhat similar system (Ru complex/amine/ethyl-2 bromoisobutyrate) was proposed, but the efficiency remains low (20–30% MMA conversion for 4 h exposure to a 25 mW/cm² Xe lamp).⁸

In the present paper, photoinitiating systems based on iridium complexes IrCs (Scheme 1), *N*-methyldiethanolamine (MDEA), and phenacylbromide (PABr) are presented as novel photocatalysts exhibiting a high efficiency in free radical polymerization (Scheme 2). Their polymerization ability will be checked. The underlying chemical mechanisms will be investigated by electron spin resonance (ESR) and luminescence experiments.

IrCs for free radical polymerization: The free radical polymerization of pentaerythritol tetraacrylate (EPT) in laminate in the presence of Ir_b/MDEA/PABr is very efficient under visible light (Figure 1A, curve 5): no inhibition time, $R_p/[M_0] = 0.245 \text{ s}^{-1}$, 60% EPT conversion within 20 s under the Xe lamp exposure. In the absence of MDEA (or PABr), the

Received: November 18, 2011

Accepted: January 6, 2012

Published: January 18, 2012

Scheme 1

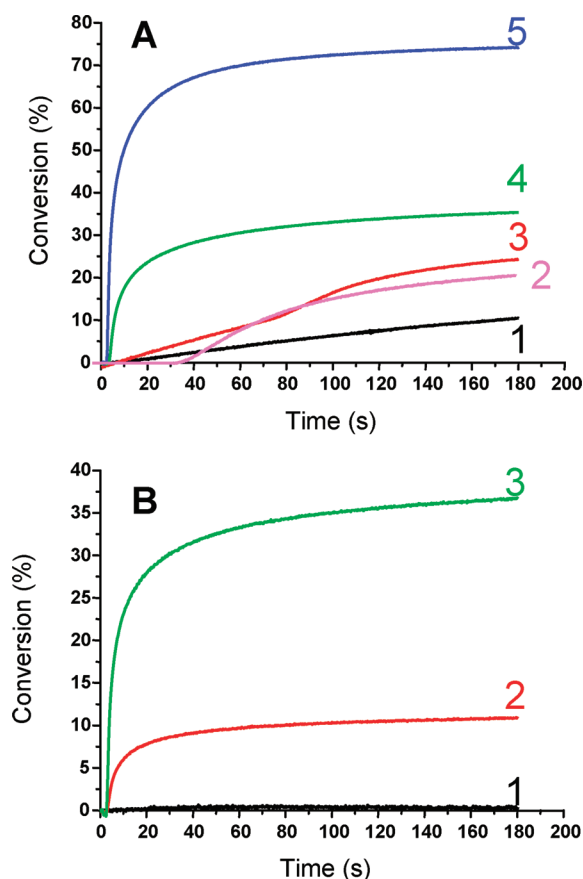
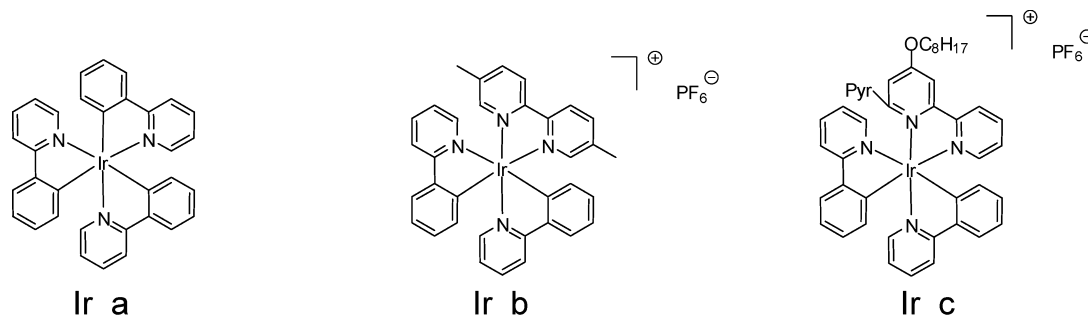


Figure 1. (A) Polymerization profiles of EPT upon a Xenon lamp irradiation ($\lambda > 390$ nm) in laminate in the presence of (1) Ir_b (0.2% w/w); (2) MDEA/PABr (4.5%/3% w/w); (3) Ir_b/PABr (0.2%/3% w/w); (4) Ir_b/MDEA (0.2%/4.5% w/w); (5) Ir_b/MDEA/PABr (0.2%/4.5%/3% w/w); (B) under air in the presence of (1) Ir_b/PABr (0.2%/3% w/w); (2) Ir_b/MDEA (0.2%/4.5% w/w); (3) Ir_b/MDEA/PABr (0.2%/4.5%/3% w/w).

efficiency drops down (Figure 1, curves 3 and 4). This highlights the role of the proposed three-component combination. For MDEA/PABr, almost no polymerization is observed also showing the importance of IrC (Figure 1, curve 2).

Using the corresponding $\text{Ru}(\text{bpy})_3^{2+}$ /MDEA/PABr reference system leads to an inhibition time = 20 s and $R_p/[M_0] \sim 0.02 \text{ s}^{-1}$.^{6a} The efficiency of the investigated IrCs decreases in the series Ir_b > Ir_c > Ir_a (Figure 1 in the SI). Remarkably, the Ir_b/MDEA/PABr three-component system is able to initiate the polymerization under air (Figure 1B, curve 3). When using a $\text{Ru}(\text{bpy})_3^{2+}$ based system, no polymerization was

observed under the same experimental conditions. All these experiments underline the high efficiency of the studied IrCs compared to $\text{Ru}(\text{bpy})_3^{2+}$. Such polymerization profiles (Figure 1) compare well with those obtained in the presence of other more conventional photoinitiating systems based on organic compounds (e.g., Eosin-Y, titanocene derivatives, thiopyrylium derivatives, etc.).^{5f}

Initiation mechanism: The IrCs are characterized by good visible light absorption properties, allowing an excellent matching with the emission spectrum of the Xenon lamp (Figure 2 in SI; $\epsilon_{400 \text{ nm}} = 4880, 3580, \text{ and } 5850 \text{ M}^{-1} \text{ cm}^{-1}$ for Ir_a, Ir_b, and Ir_c, respectively). The relative absorbed light intensity evaluated from the overlap of the absorption of the IrCs with the emission spectrum (as done in other papers¹²) are in a 1.4, 1, and 1.9 ratio for Ir_a, Ir_b, and Ir_c, respectively. These ratios do not parallel the efficiency of the IrCs (Ir_b > Ir_c > Ir_a), showing that other factors must be taken into account for a discussion of the polymerization initiating ability of the three-component systems.

The three-component system: ESR-ST and luminescence investigation: Upon a visible light irradiation of IrC or IrC/PABr solutions, no free radical is observed in ESR spin trapping experiments (Figure 2). Using IrC/MDEA, the signal remains

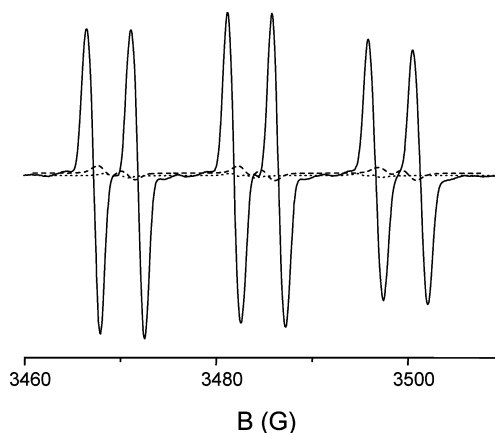


Figure 2. ESR spectra obtained after a blue LED bulb irradiation (30 s) of Ir_b/PABr (dot line), Ir_b/MDEA (dash line), and Ir_b/MDEA/PABr (full line) in *tert*-butylbenzene/acetonitrile. Phenyl-*N*-*t*-butylnitron (PBN) is used as spin-trap.

rather weak: the PBN spin adduct ($a_N = 14.5 \text{ G}$; $a_H = 2.5 \text{ G}$) is assigned to the aminoalkyl radical (A^\bullet) produced in (1a-b). Interestingly, in IrC/MDEA/PABr, a very strong signal of the PBN spin adduct is observed ($a_N = 14.9 \text{ G}$; $a_H = 4.6 \text{ G}$); it is confidently ascribed to a phenacyl radical¹³ formed as in

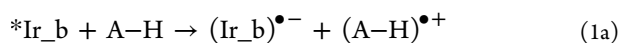
reaction 2. The reduction potential of PABr (-0.78 V vs SCE)¹⁴ is higher than the oxidation potentials of the different Ir^{•-} (Table 1): reaction 2 is therefore a thermodynamically

Table 1. for the Different Investigated Ir Complexes: Luminescence Lifetimes under Argon (τ_0), Reduction Potentials (E_{red}), Excited State Energy Levels (E_T), Interaction Rate Constants of the Luminescent State with MDEA in Acetonitrile and ΔG for Reaction 1a

	τ_0 (ns)	E_{red} (V vs SCE)	E_T^b eV	ΔG^c eV	k (MDEA) $M^{-1} s^{-1}$
Ir_a	1300 ^a	$\leftarrow 2$	2.5 ^a	> 0.3	$< 5 \times 10^6$
Ir_b	890 ^a	-1.65	2.6 ^a	-0.15	2.5×10^7 ; $(3.4 \times 10^7)^d$
Ir_c	78	-1.50	2.45	-0.15	1.05×10^7

^aFrom ref 7. ^bEvaluated from the luminescence band edge, as presented in ref 7. ^c $\Delta G = E_{\text{ox}} - E_{\text{red}} - E_T$; calculated from the classical Rehm–Weller equation, where E_{ox} , E_{red} , and E_T are the oxidation potential of the donor, the reduction potential of the acceptor, and the excited state energy. $E_{\text{red}} = 0.8$ V was used for MDEA (this work). ^dFor ethyldimethylaminobenzoate.

favorable process.



The rate constants ($k_{(1a)}$) of reaction 1a were determined from the quenching of the luminescent excited states by MDEA (Table 1; Figure 3). The $k_{(1a)}$ s are strongly affected by the IrC structure, that is, ranging from $< 0.5 \times 10^7 M^{-1} s^{-1}$ for Ir_a to $2.5 \times 10^7 M^{-1} s^{-1}$ for Ir_b. The formation of A[•] ascribed to (reaction 1b) is presumably a slow process as the protons can hardly be trapped in the medium (contrary to the case of, e.g., a ketone/amine interaction). As the aminoalkyl radicals present excellent polymerization initiating properties,¹⁵ Ir_b/MDEA appears, however, as a better initiating system than Ir_b alone (Figure 1A, curve 4 vs curve 1). On the opposite in IrC/MDEA/PABr, reaction 2 is clearly the driving reaction for the production of the initiating radicals (R[•]), with reaction 1b contributing to some extent. The overall mechanism is presented in Scheme 3.

Role of the IrCs: As shown above, the IrC activity in the IrC/MDEA/PABr systems decreases in the series Ir_b > Ir_c > Ir_a. This behavior can be ascribed to the reduction ability of the different iridium complexes, that is, the $k_{(1a)}$ s also decrease in this series (Table 1). The free energy changes for reaction 1a calculated from the classical Rehm–Weller equation¹⁶ (Table 1) support an electron transfer process, that is, $\Delta G < 0$ for Ir_b and Ir_c. For Ir_a, $k_{(1a)}$ is lower than for the other IrCs in agreement with a less favorable ΔG .

These results also underline the importance of the IrC luminescent state lifetime (τ_0); that is, for Ir_b and Ir_c, the $k_{(1a)}$ s are quite similar, but the polymerization efficiency is much better for Ir_b than for Ir_c (Figure 1 in SI). This behavior is ascribed to the rather short lifetime of the ^{*}Ir_c

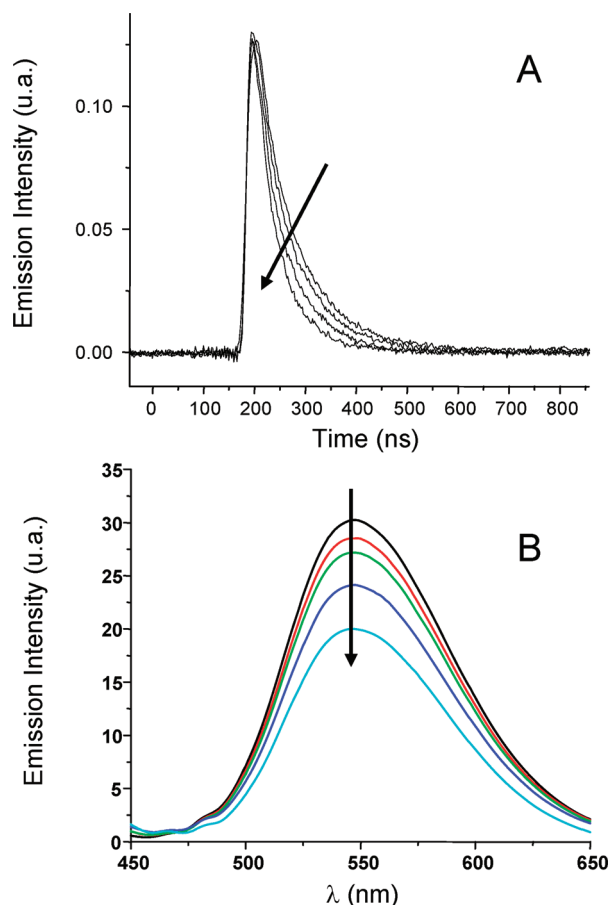
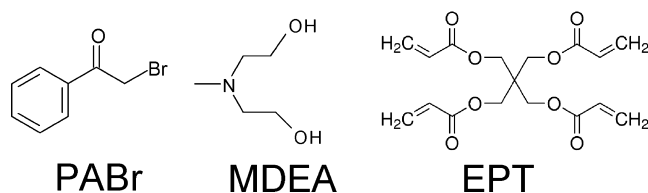
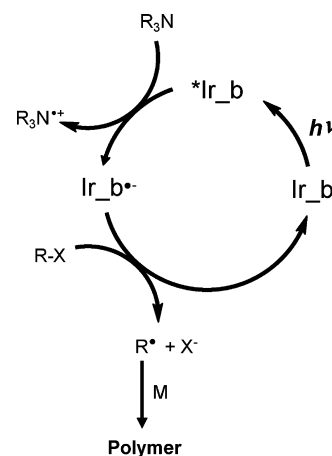


Figure 3. (A) Luminescence decay curves of Ir_c monitored at 550 nm for different [MDEA] (from 0 to 0.84 M); degassed (argon) acetonitrile; excitation at 355 nm. (B) Luminescence spectra of Ir_b in acetonitrile for [ethyldimethylaminobenzoate] = 0–0.4 M.

Scheme 2



Scheme 3



excited state (i.e., $\tau_0 = 78$ ns for Ir_c vs $\tau_0 = 890$ ns for Ir_b; Table 1), which ensures a less favorable reaction 1a process. The quantum yields $\Phi_{(1a)}$ for reaction 1a evaluated according to eq 3 are 0.89 and 0.23 for Ir_b and Ir_c, respectively. This accounts for the difference in the IrC activity observed for the free radical polymerization initiation.

$$\Phi_{(1a)} = k_{(1a)}[\text{MDEA}]/(1/\tau_0 + k_{(1a)}[\text{MDEA}]) \quad (3)$$

Photoluminescence of the polymer films: Interestingly, the formed polymer using a IrC/MDEA/PABr initiating system exhibits excellent photoluminescence properties (Figure 3 in SI); the luminescence intensity of Ir_b does not decrease during the polymerization. This is in agreement with the photocatalyst behavior of the Ir complexes, that is, these compounds are both involved in the photoinitiation step and regenerated, thereby leading to a photoluminescence of the formed polymers. These results highlight the dual role of the photocatalyst as (i) a photosensitizer and (ii) an in situ incorporated photoluminescent compound. Such a behavior was also recently reported for IrCs used in an oxidative cycle to initiate the cationic ring-opening photopolymerization of epoxy monomers.⁷

In the present paper, three iridium complexes IrCs are proposed as photocatalysts for acrylate free radical polymerization. The selected ligands strongly affect the IrC behavior. For the first time, high performance photoinitiating systems under visible light exposure are thus achievable now using either a reduction cycle (as here) or an oxidation cycle (as in ref 7). For a given amine and halide, the key parameters that govern the polymerization rates are the reduction ability of the excited states (*Ir) as well as the excited state lifetimes. The luminescence properties of the formed polymers by free radical polymerization deserve to be investigated, for example, for OLEDs applications.¹⁰ The development of other IrCs and new IrC/additive1/additive2 three-component systems for free radical polymerization, FRPCP and manufacture of interpenetrated polymer networks (IPN) will be presented in forthcoming papers.

EXPERIMENTAL SECTION

(i) Iridium(III) complexes: Tris[2-phenylpyridinato-*C*²,*N*]iridium(III) (Ir_a) was purchased from Aldrich and used as received. [(5-*S*'dimethyl-2,2'-bipyridine)-bis-(2-phenylpyridine)-iridium(III)] hexafluorophosphate (Ir_b) was synthesized according to a previous literature procedure.⁷ (4"-Octyloxy-2,2':6',2"-terpyridine)-bis-(2-phenylpyridine)-iridium(III)] hexafluorophosphate (Ir_c) was prepared in one step by a bridge-splitting and substitution reaction of the μ -dichlorobridged iridium dimer Ir₂(ppy)₄Cl₂ with 2 equiv of 4"-octyloxy-2,2':6',2"-terpyridine. All iridium(III) complexes Ir_a-Ir_c are stable in air.

Procedure for the synthesis of Ir_c: Ir₂(ppy)₄Cl₂ (0.5 g, 0.466 mmol) and 4"-octyloxy-2,2':6',2"-terpyridine⁹ (336 mg, 0.932 mmol, 2 equiv) were suspended in a mixture of MeOH (30 mL) and chloroform (30 mL). The reaction was refluxed under argon for 48 h in the dark. After cooling, the solution was concentrated to 1/3 of its initial volume. Metathesis with an aqueous solution of potassium hexafluorophosphate precipitated a yellow solid that was filtered off, washed with water, and dried in vacuum. The crude product was purified by dissolution in a minimum of acetone and precipitation with pentane. The yellow powder was filtered off, washed with pentane, and dried in vacuum (889 mg, 95% yield). Complex Ir_c was obtained as a mixture of two geometrical stereoisomers as a result of the two potential orientations of the noncoordinated pyridine.¹⁰

¹H NMR (400 MHz, CDCl₃, ppm): 0.88 (t, 3H, *J* = 7.0 Hz), 1.15–1.55 (m, 10H), 1.83 (qt, 2H, *J* = 8.4 Hz), 4.28 (t, 2H, *J* = 6.3 Hz), 5.44

(d, 1H, *J* = 7.5 Hz), 5.87 (d, 1H, *J* = 7.4 Hz), 6.26 (t, 1H, *J* = 7.2 Hz), 6.46 (d, 1H, *J* = 7.7 Hz), 6.55 (t, 1H, *J* = 7.3 Hz), 6.68 (t, 1H, *J* = 7.4 Hz), 6.83–6.87 (m, 2H), 6.99–7.06 (m, 2H), 7.13 (td, 1H, *J* = 7.4 Hz, *J* = 1.2 Hz), 7.23–7.35 (m, 3H), 7.43 (d, 1H, *J* = 7.3 Hz), 7.52 (d, 1H, *J* = 7.3 Hz), 7.69–7.88 (m, 5H), 8.02–8.03 (m, 1H), 8.10 (td, 1H, *J* = 8.1 Hz, *J* = 1.2 Hz), 8.16 (d, 1H, *J* = 4.7 Hz), 8.58–8.69 (m, 2H), 8.77 (d, 1H, *J* = 5.5 Hz). ¹³C NMR (100 MHz, CDCl₃, ppm): 13.95, 13.99, 22.2, 22.5, 25.6, 28.6, 29.0, 29.1, 30.8, 31.6, 34.0, 68.1, 69.9, 107.3, 110.3, 115.3, 119.0, 119.1, 120.4, 121.2, 122.38, 122.41, 122.56, 122.59, 123.6, 123.7, 123.8, 125.5, 127.4, 129.7, 130.3, 130.5, 132.0, 135.9, 136.7, 137.9, 138.0, 139.4, 142.1, 142.8, 146.7, 147.9, 148.9, 149.7, 150.0, 151.7, 155.7, 156.0, 156.6, 156.9, 158.6, 163.7, 166.6, 167.2, 168.0. HRMS: [M]⁺* calcd, 862.3091; found, 862.3088

(ii) Polymerization procedures: *N*-Methyldiethanolamine (MDEA) and phenacylbromide (PABr) were obtained from Aldrich and used with the best purity available (Scheme 2). Pentaerythritol tetraacrylate (EPT from Cytec) was selected as a standard acrylic monomer (Scheme 2).

The three-component photoinitiating systems are based on Ir_a (Ir_b or Ir_c)/MDEA/PABr (0.2/4.5/3% w/w). The evolution of the double bond content was continuously followed by real-time FTIR spectroscopy at about 1630 cm⁻¹, as presented in refs 6 and 7. Maximum polymerization rates (*R_p*) were evaluated from the polymerization profiles; as usual, *R_p*/[M₀] are given with [M₀] as the initial monomer concentration. Xenon lamp exposure was used for these photopolymerization processes ($\lambda > 390$ nm, intensity: 60 mW/cm²).

(iii) ESR experiments: ESR spin-trapping (ESR-ST) experiments were carried out using a X-Band EMX-plus spectrometer (Bruker Biospin). The radicals were produced at RT under a Xenon lamp irradiation (Hamamatsu; filtered for $\lambda > 390$ nm) and trapped by phenyl-*N*-t-butylnitron (PBN) according to a procedure described in detail in ref 11.

(iv) Luminescence lifetimes and quenching: The luminescence lifetime for Ir_c was determined with an Edinburgh LP900 laser flash photolysis in emission mode. The emission spectra were recorded in acetonitrile (FP-750; JASCO).

(v) Redox potentials: The redox potentials were measured in acetonitrile by cyclic voltammetry with tetrabutylammonium hexafluorophosphate (0.1 M) as a supporting electrolyte (Voltalab 6 Radiometer; the working electrode was a platinum disk and the reference a saturated calomel electrode-SCE). Ferrocene was used as a standard and the potentials determined from the half peak potential were referred to the reversible formal potential of this compound.

ASSOCIATED CONTENT

Supporting Information

Additional figures. This material is available free of charge via the Internet at <http://pubs.acs.org>.

AUTHOR INFORMATION

Corresponding Author

*E-mail: j.lalevee@uha.fr; didier.gigmes@univ-provence.fr.

Notes

The authors declare no competing financial interest.

ACKNOWLEDGMENTS

This work was supported by the "Agence Nationale de la Recherche" Grant ANR 2010-BLAN-0802. J.L. thanks the Institut Universitaire de France for financial support.

REFERENCES

- (1) (a) Nicewicz, D. A.; MacMillan, D. W. C. *Science* **2008**, *322*, 77–80. (b) Nagib, D. A.; Scott, M. E.; MacMillan, D. W. C. *J. Am. Chem. Soc.* **2009**, *131*, 10875–10877. (c) Shih, H.-W.; Vander Wal, M. N.; Grange, R. L.; MacMillan, D. W. C. *J. Am. Chem. Soc.* **2010**, *132*, 13600–13603.

(2) (a) Zeitler, K. *Angew. Chem., Int. Ed.* **2009**, *48*, 9785–9789. (b) Narayanam, J. M. R.; Stephenson, C. R. J. *Chem. Soc. Rev.* **2011**, *40*, 102–113. (c) Dai, C.; Narayanam, J. M. R.; Stephenson, C. R. J. *Nature Chem.* **2011**, *3*, 140–145. (d) Nguyen, J. D.; Tucker, J. W.; Konieczynska, M. D.; Stephenson, C. R. J. *J. Am. Chem. Soc.* **2011**, *133*, 4160–4163.

(3) (a) Ischay, M. A.; Lu, Z.; Yoon, T. P. *J. Am. Chem. Soc.* **2010**, *132*, 8572–8574. (b) Du, J.; Yoon, T. P. *J. Am. Chem. Soc.* **2009**, *131*, 14604–14605. (c) Yoon, T. P.; Ischay, M. A.; Du, J. *Nature Chem.* **2010**, *2*, 527–532.

(4) (a) Dietliker, K. *A Compilation of Photoinitiators Commercially Available for UV Today*; Sita Technology Ltd.: London, 2002; (b) Fouassier, J. P.; Lalevée, J. *Photoinitiators for Polymer Synthesis: Scope, Reactivity and Efficiency*; Wiley-VCH: Weinheim, to be published.

(5) (a) Fouassier, J. P. *Photoinitiation, Photopolymerization, Photocuring*; Hanser: München, 1995; (b) Davidson, S. *Exploring the Science, Technology and Application of UV and EB Curing*; Sita Technology Ltd.: London, 1999; (c) Neckers, D. C. *UV and EB at the Millenium*; Sita Technology: London, 1999; (d) *Photoinitiated Polymerization*, Belfied, K. D., Crivello, J. V. Eds.; ACS Symposium Series 847; American Chemical Society: Washington DC, 2003; (e) *Basics of Photopolymerization Reactions*; Fouassier, J. P., Allonas, X., Eds.; Research Signpost: Trivandrum India, 2010; (f) Lalevée, J.; Tehfe, M. A.; Morlet-Savary, F.; Alloas, X.; Graff, B.; Fouassier, J. P. *Progress Org. Coat.* **2011**, *70*, 83–90.

(6) (a) Lalevée, J.; Blanchard, N.; Tehfe, M. A.; Morlet-Savary, F.; Fouassier, J. P. *Macromolecules* **2010**, *43*, 10191–10195. (b) Lalevée, J.; Blanchard, N.; Tehfe, M. A.; Peter, M.; Morlet-Savary, F.; Fouassier, J. P. *Macromol. Rapid Commun.* **2011**, *32*, 917–920. (c) Lalevée, J.; Blanchard, N.; Tehfe, M. A.; Peter, M.; Morlet-Savary, F.; Gigmès, D.; Fouassier, J. P. *Polym. Chem.* **2011**, *2*, 1986–1991. (d) Lalevée, J.; Blanchard, N.; Tehfe, M. A.; Peter, M.; Morlet-Savary, F.; Fouassier, J. P. *Polym. Bull.* **2012**, *68*, 341–347.

(7) Lalevée, J.; Peter, M.; Dumur, F.; Gigmès, D.; Blanchard, N.; Tehfe, M. A.; Morlet-Savary, F.; Fouassier, J. P. *Chem.–Eur. J.* **2011**, *17*, 15027–15031.

(8) Zhang, G.; Song, I. Y.; Ahn, K. H.; Park, T.; Choi, W. *Macromolecules* **2011**, *44*, 7594–7599.

(9) Nielsen, P.; Toftlund, H.; Bond, A. D.; Boas, J. F.; Pilbrow, J. R.; Hanson, G. R.; Noble, C.; Riley, M. J.; Neville, S. M.; Moubaraki, B.; Murray, K. S. *Inorg. Chem.* **2009**, *48*, 7033–7047.

(10) Dumur, F.; Guillaneuf, Y.; Guerlin, A.; Wantz, G.; Bertin, D.; Miomandre, F.; Clavier, G.; Gigmès, D.; Mayer, C. R. *Macromol. Chem. Phys.* **2011**, *212*, 1616–1628.

(11) (a) *Landolt Bornstein: Magnetic Properties of Free Radicals*; Fischer, H., Ed.; Springer Verlag: Berlin, 2005; Vol. 26d; (b) Chandra, H.; Davidson, I. M. T.; Symons, M. C. R. *J. Chem. Soc., Faraday Trans. 1* **1983**, *79*, 2705–2711. (c) Criqui, A.; Lalevée, J.; Allonas, X.; Fouassier, J. P. *Macromol. Chem. Phys.* **2008**, *209*, 2223–2231.

(12) Lalevée, J.; El-Roz, M.; Morlet-Savary, F.; Graff, B.; Alonas, X.; Fouassier, J. P. *Macromolecules* **2007**, *40*, 8527–8530.

(13) Barclay, L. R. C.; Cromwellan, G. R.; Hilborn, J. W. *Can. J. Chem.* **1994**, *72*, 35–41.

(14) Renaud, J.; Scaiano, J. C. *Can. J. Chem.* **1996**, *74*, 1724–1730.

(15) Lalevée, J.; Graff, B.; Allonas, X.; Fouassier, J. P. *J. Phys. Chem. A* **2007**, *111*, 6991–6998.

(16) Rehm, D.; Weller, A. *Isr. J. Chem.* **1970**, *8*, 259–271.